Electronic Supplementary Material (ESI) for New Journal of Chemistry.
This journal is © The Royal Society of Chemistry and the Centre National de la Recherche Scientifique 2019

Exploring Binding plus Cleavage activities of Nickel^{II} complexes towards DNA and Proteins

Manish Kumar[a], Neetika Lal[b], Pratibha Mehta Luthra[b] and Dhanraj T. Masram[a]*

[a]Department of Chemistry, University of Delhi, Delhi-110007, India

[b]Dr. B.R. Ambedkar Centre for Biomedical Research, University Of Delhi Delhi-110007, India

Supplementary material file

*Corresponding author: *E-mail*; ***dhanraj_masram27@rediffmail.com***; Tel.; +91-11-27666646

TABLE OF CONTENTS

1. Experimental Details

1.1.Materials and Apparatus

Nalidixic acid, 2,2'-bipyridine (=bpy), 1,10-phenanhroline (=phen), 8-hydroxyquinoline (=8-Hq), NaOH, $NiCl_2.6H_2O$, NaCl, trisodium citrate, CT DNA, EtBr, BSA and HSA were purchased from Sigma-Aldrich Co., and supercoiled plasmid DNA (pBR322), Agarose, Acrylamide/Bis-acrylamide, sodium lauryl sulphate (sodium dodecyl sulphate, SDS), ammonium per sulphate (APS), N,N,N′,N′-Tetramethylethylenediamine (TEMED) was purchased from SRL Diagnostics. All the chemicals and solvents used in the present study were reagent grade and used without any further purification. Doubly distilled water was used to prepare the buffer solutions and the pH was maintained by titration with 0.1 M NaOH solution. Microanalysis for carbon, hydrogen and nitrogen was carried out using a GMBH Vario EL−III spectrometer analyzer. Fourier-transform infrared (FT-IR) spectrum was performed on Thermo Fisher FT-IR spectrometer (NICOLET iS50). The UV/Vis absorption spectra were recorded in solution on a LABINDIA UV/VIS spectrophotometer (UV-3092) using a quartz cells of 1 cm path length. The magnetic properties of synthesized complexes were studied using vibrating sample magnetometer (VSM) (Microsense, Model ADE-EV9) at room temperature in the applied field of 15 kOe. All fluorescence measurements were performed on a Cary Eclipse Fluorescence spectrophotometer. The viscosity measurements of the samples were acquired on an ALPHA L Fungilab rotational viscometer device at room temperature (rt). Circular dichroism spectra of the complexes with CT DNA as well as proteins solution were obtained with a JASCO CD-Spectropolarimeter (J-815) with 150W Xe lamp under nitrogen flush at 25ºC. Electrochemical measurements were carried out on a CHI604D electrochemical analyzer in a 30 mL three-electrode electrolyte cell. The melting point (mp) of complexes were acquired with a Lab India melting point tool.

1.2. Synthetic procedure of mixed ligands Nickel(II) complexes

Synthesis of [Ni(nal)$_2$bpy], 1a: A warm methanol solution containing nalidixic acid (Hnal = $C_{12}H_{12}N_2O_3$) (187 mg, 0.8 mmol) and NaOH (16 mg, 0.4 mmol) was continuously stirred until a clear solution was obtained. Afterwards, a methanolic solution of $Ni(OCOCH_3)_2.4H_2O$ (100 mg, 0.4 mmol) was simultaneously added to the solution mixture and a light green color solution was formed. After 1 h stirring, a solution of bpy (63 mg, 0.4 mmol) was dropwise added and then the reaction mixture was refluxed for 2 h at 60 ºC. After the completion of

reaction the resultant solution was filtrated to remove any solid impurities and vapour diffusion technique was used for growing crystals. After 5-6 days, green crystals of **1a** were collected that is suitable for X-ray structure determination. Yield: 70% (0.19 g), mp: 310-312ºC. Anal. Calcd for $C_{34}H_{30}N_6NiO_6$, requires: C, 60.29; H, 4.46; N, 12.41. found: C, 60.17; H, 4.42; N, 12.37. FT-IR resonances: (ν_{max}, cm^{-1}); $(C=O)_{py}$ 1619 (*vs*); $(CO_2)_a$ 1563 (s); $(CO_2)_s$ 1351 (s); Δ value = 212 cm^{-1}. Electronic spectrum [λ_{max}, nm (ε, $M^{-1}cm^{-1}$)]: (in DMSO) 262 (40,921), 318(29,300).

Synthesis of [Ni(nal)$_2$phen], 1b: This complex was synthesized following the above procedure used for **1a**, except that 1,10-phenanthroline (phen = $C_{12}H_8N_2$) (72 mg, 0.4 mmol) was used in place of 2,2'-bipyridine ligand (bpy = $C_{10}H_8N_2$). Light green colored crystals of **1b** obtained in the reaction mixture which is suitable for X-ray structure determination. Yield: 70% (0.19 g), mp: 306-308ºC. Anal. Calcd for $C_{36}H_{30}N_6NiO_6$, requires: C, 61.65; H, 4.31; N, 11.98. found: C, 61.47; H, 4.22; N, 11.67. FT-IR resonances: (ν_{max}, cm^{-1}); $(C=O)_{py}$ 1610 (*vs*); $(CO_2)_a$ 1549 (s); $(CO_2)_s$ 1336 (s); Δ value = 213 cm^{-1}. Electronic spectrum [λ_{max}, nm (ε, $M^{-1}cm^{-1}$)]: (in DMSO) 262 (37,672), 325(12,738).

Synthesis of [Ni(8-Hq)$_2$bpy], 1c: To a solution of $Ni(OCOCH_3)_2.4H_2O$ (100 mg, 0.4 mmol) in methanol (10 mL) were added the 8-hydroxyquinlone (8-Hq = C_9H_7NO) (116 mg, 0.8 mmol) and the reaction mixture was refluxed for 1 h. After that a solution of 2,2'-bipyridine ligand (bpy = $C_{10}H_8N_2$) (63 mg, 0.4 mmol) was simultaneously added and further refluxed for 1 h. After the completion of reaction, the mixture was allowed to cool at rt and then filtrated to remove any solid particles and kept for slow evaporation of the methanol solution. Dark brown crystals of **1c** were found to be suitable for X-ray structure studies. Yield: 70% (0.19 g), mp: 258-260ºC. Anal. Calcd for $C_{28}H_{20}N_4NiO_2$, requires: C, 66.84; H, 4.01; N, 11.13. found: C, 66.77; H, 3.92; N, 11.07. FT-IR resonances: (ν_{max}, cm^{-1}); (C−N) 1572 (*vs*). Electronic spectrum [λ_{max}, nm (ε, $M^{-1}cm^{-1}$)]: (in DMSO) 262 (24,194), 297 (10,482), 335 (3,160) 407 (2,308).

1.3. X-ray crystallographic

Suitable single crystals of complexes with appropriate dimensions of 0.08×0.06×0.05 mm^2 in **1a**, 0.14×0.09×0.05 mm^2 in **1b** and 0.22×0.19×0.12 mm^2 in **1c** were selected using microscope and mounted on a Mitgen Cryoloop in a random angle. The crystallographic data of complexes were carried out by using an Oxford XCalibur CCD diffractometer equipped with graphite monochromatic Mo Kα radiation (λ = 0.71073 Å).[1] The structures of complexes were solved by direct methods of ShelXT with the help of Olex2 program and refined by ShelXL 2018/3.[2]

All non-hydrogen atoms were refined anisotropically and located H-atoms at their expected position to the carbon atoms in complexes (**1a**, **1b** and **1c**) by using riding-hydrogen model. The molecular graphics and data analysis of bond angles, bond lengths and intermolecular interactions were done with Mercury and Platon programs.[3] The crystallographic data collection as well as the structural refinement data for complexes **1a-1c** are summarized in Supporting Information Table S1.

1.4. DNA binding and DNA cleavage studies

All of the experiments involving binding and cleavage activities of compounds with CT DNA were carried out by using the procedure as described by us previously.[4]

1.5. Proteins binding and Proteins cleavage studies

The proteins binding and cleavage studies of compounds were carried out by employing the procedure as described by us previously.[4]

1.6. In vitro cytotoxicity assay

Cytotoxicity studies of the complexes **1a-1c** along with standard drug cisplatin were carried out on human lung cells (A-549) and human breast cells (MCF-7) using the MTT assay method.[5] The A-549 and MCF-7 cancer cells were grown in Dulbecco's Modified Eagle Medium (DMEM) containing 10% fetal bovine serum (FBS) along with 100 μg/mL streptomycin and 100 units per mL penicillin at 37ºC under a humidified atmosphere of 5% CO_2. For the screening test, the cells were seeded in a 96-well cell culture plates and incubated at 37 ºC for 24 h under a conditions of 5% CO_2, 95% air and 100% relative humidity prior to the addition of complexes. The complexes **1a-1c** were dissolved in DMSO and again diluted in the respective medium containing 1% FBS. After that, the cells were treated with changing concentrations of complexes and incubated at 37 ºC for 24 h. After 24 h, the MTT (0.5 μg/mL) was added to each well for 4 h incubation. The medium with MTT was then flicked off and formation of formazans which dissolved in 100 μL DMSO. The absorbance was then recorded at 540 nm with a reference wavelength of 690 nm. The IC_{50} values of the compounds were determined by using the graph of the percentage (%) of survival cells *versus* the concentrations (μg/mL) of the complexes.[6,7] Triplication was maintained, and the medium not containing the complexes served as the control.

2. Bioassays

2.1. Stern-Volmer equation for SAs quenching studies

To obtain a deep insight into the quenching progression ,the values of Stern-Volmer quenching (K_{SV}, M^{-1}) and the quenching constant (k_q, $M^{-1}s^{-1}$) for the interaction of complexes **1a-1c** with SAs have been evaluated according to Stern-Volmer eqn S1.[8,9]

$$I_o/I = 1 + K_{SV}[Q] = 1 + k_q\tau_0[Q] \quad \text{(eq. S1)}$$

Herein, K_{SV} (M^{-1}) represents the Stern-Volmer quenching and it is obtained by the slope of the diagram I_0/I vs [Q], I and I_o denoted the fluorescence intensities of SAs in the bound of the complexes and in the free form respectively, [Q] is the concentration of the complexes. The value of quenching rate constant (k_q, $M^{-1}s^{-1}$) was obtained according to the eqn S2.

$$K_{SV} = k_q\tau_0 \quad \text{(eq. S2)}$$

Herein, τ_0 is the average lifetime of SAs in the absence of the quencher and taking at 10^{-8} s.

2.2. Scatchard equation for SAs quenching studies

According to the Scatchard eqn S3.[10]

$$log\left[{(I_0 - I)}/{I}\right] = logK_b + nlog[Q] \quad \text{(eq. S3)}$$

the values SAs binding constant (K_b M^{-1}) and the number of binding sites per albumins (n) were calculated from the slope and intercept in the linear plots of $log[(I_0 - I)/I]$ *versus* $log[Q]$.

2.3. Calculation of binding parameters (ΔH^o,$\Delta S^o$and ΔG^o**)**

The enthalpy change (ΔH^o) and entropy change (ΔS^o) can be calculated according to the van't Hoff eqn S4.[11,12]

$$logK_b = -\frac{\Delta H^o}{2.303RT} + \frac{\Delta S^o}{2.303R} \quad \text{(eq. S4)}$$

Herein, K_b is the binding constant at different temperature, R is the ideal gas constant and T represents the experimental temperature (25, 30 and 35ºC). The values of $\Delta H^o$and ΔS^owere obtained from the linear plots of $logK_b$ versus$1/T$. If the temperature were slightly changes, the enthalpy change (ΔH^o) can be regarded as a constant. The free energy change (ΔG^o) can be evaluated by making use of the binding constants at three different temperatures according to the following eqn S5.

$$\Delta G = -RTlnK = \Delta H^o - T\Delta S^o \quad \text{(eq. S5)}$$

2.4. CD spectroscopy

The $\alpha-$ helix (%) content of free SAs and in the presence of complexes **1a-1c** were calculated at 224 nm by the following eqn S6.[13,14]

$$MRE_{224} = {observed\ CD\ (m\ \text{deg})}/{C_P \times n \times l \times 10} \qquad \text{(eq. S6)}$$

Here, C_P is the proteins (BSA/HSA) concentration in moles dm^{-1}, n is the number of amino acid residues (583 for BSA and 585 for HSA) and l is the path length of the cell (1 cm).

The percentage (%) of Helicity was calculated from the mean MRE value observed at 224 nm, according to the following eqn S7.

$$\alpha - helix\ (\%) = {-MRE_{224} - 4000}/{33000 - 4000} \times 100 \qquad \text{(eq. S7)}$$

Here, MRE_{224} represents the mean residue elasticity (in deg cm^2 $dmol^{-1}$) values in observed at 224 nm, 4000 represents is the MRE value of the β-form and random coil conformation at 224 nm, and 33 000 is the value of MRE of a pure α-helix at 224 nm.

2.5. DNA binding study

The binding constants (K_b) were determined from the titration results by the Wolf-Shimer eqn S8.[15]

$$[DNA]/(\varepsilon_A - \varepsilon_f) = [DNA]/(\varepsilon_A - \varepsilon_f) + 1/K_b(\varepsilon_b - \varepsilon_f) \qquad \text{(eq. S8)}$$

Where, [DNA] is the concentration of DNA in base pair, ε_b is the absorption coefficient of the complexes fully bounded to CT DNA, ε_f is the extinction coefficient for the free complexes and ε_A is apparent absorption coefficient and is observed from A_{obsd}/[complexes]. The binding constant, K_b of the complexes **1a-1c** are calculated by the ratio of slope to the y-intercept by the linear fitting plots of $[DNA]/(\varepsilon_A - \varepsilon_f)$ *versus* [DNA] according to the above equation.

2.6. Stern-Volmer equation for EtBr competitive study

The quenching efficiency for complexes **1a-1c** were analyzed according to the following Stern-Volmer eqn S9.[16]

$${I_0}/{I} = 1 + K_{SV}[Q] \qquad \text{(eq. S9)}$$

Where, I_0 and I are the emission intensities in the absence and the presence of the quencher (complexes), respectively. $[Q]$ is the concentration of the quencher and K_{SV} is the quenching

constant and it is obtained from the slope of the linear plots of I_0/I *versus* $[Q]$ (Stern-Volmer plots, Supporting Information Fig. S21)

2.7. Apparent binding constant (K_{app})

Further, apparent binding constant (K_{app}) of complexes were calculated by using the following eqn S10.[17]

$$K_{EtBr}[EtBr] = K_{app}[\text{Complex}] \quad \text{(eq. S10)}$$

Herein, [complex] corresponding to the concertation of the complexes at 50% reduction in the emission intensity of EtBr, [EtBr] is the concertation of EtBr = 10 μM and K_{EtBr} = 1.0 × 10^7, $M^{-1.}$

3. Supporting Tables and Figures

Table S1. Crystallographic Data and Structure Refinement parameters for complexes **1a-1c**.

	1a	**1b**	**1c**
Empirical Formula	$C_{35}H_{33}N_6NiO_8$	$C_{37}H_{38}N_6NiO_{11}$	$C_{29}H_{26}N_4NiO_4$
Formula weight	724.38	801.44	553.25
Crystal system	triclinic	monoclinic	triclinic
Space group	P-1	C2/c	P-1
color	Greenish	green	brownish
a/Å	9.9515(8)	14.3041(18)	8.0970(15)
b/Å	13.1974(6)	25.146(2)	9.8370(14)
c/Å	14.5739(9)	11.4595(15)	15.489(2)
α/°	107.700(5)	90	98.035(11)
β/°	107.784(7)	111.123(14)	95.492(14)
γ/°	90.638(5)	90	93.658(14)
Volume/$Å^3$	1724.9(2)	3844.8(8)	1212.3(3)
Z	2	4	2
ρ_{calc}/gcm^{-3}	1.395	1.385	1.516
μ/mm^{-1}	0.623	0.572	0.846
F(000)	754.0	1672.0	576.0
Crystal size/mm^3	0.08×0.06×0.05	0.14×0.09×0.05	0.22×0.19×0.12
Radiation	MoKα/λ = 0.71073	MoKα/λ = 0.71073	MoKα/λ = 0.71073
2Θ range for data collection/°	7.406 to 59.082	6.75 to 59.226	6.83 to 59.782
Reflections collected	25902	28234	17832
Final R indexes [I>=2σ(I)]	R_1 = 0.0595 wR_2 = 0.1483	R1 = 0.0769 wR_2 = 0.1912	R1 = 0.0946 wR_2 = 0.2327
Final R indexes (all data)	R_1 = 0.0879, wR_2 = 0.1696	R_1 =0.1048, wR_2 = 0.2285	R1 = 0.1384 wR_2 = 0.2876
Largest diff. peak/hole/ e $Å^{-3}$	1.64/-0.53	1.27/-0.92	1.30/-1.23
Data/restraints/parameters	8265/0/482	4896/0/259	6103/0/348
Goodness-of-fit on F^2	1.034	1.040	1.017

Table S2. Selected bond distances and angles for complex **1a**.

Bond distances (Å)			
Ni(1)−N(2)	2.069(2)	Ni(1)−N(1)	2.055(2)
Ni(1)−O(1)	2.0382(19)	Ni(1)−O(4)	2.079(2)
Ni(1)−O(2)	2.032(2)	Ni(1)−O(5)	2.045(2)
C(11)−O(2)	1.263(3)	C(23)−O(5)	1.256(3)
C(1)−O(3)	1.235(4)	C(23)−O(6)	1.251(4)
Bond angles (º)			
O(2)−Ni(1)−O(1)	87.03(8)	O(5)−Ni(1)−N(1)	91.22(9)
O(1)−Ni(1)−O(5)	88.40(8)	O(2)−Ni(1)−O(4)	86.39(8)
O(1)−Ni(1)−N(1)	174.06(9)	O(2)−Ni(1)−O(5)	171.42(7)
O(1)−Ni(1)−N(2)	95.13(9)	O(1)−Ni(1)−O(4)	91.31(8)
O(2)−Ni(1)−N(1)	94.08(9)	N(2)−Ni(1)−O(4)	172.45(8)
O(2)−Ni(1)−N(2)	90.00(9)	N(1)−Ni(1)−O(4)	94.58(9)
O(5)−Ni(1)−O(4)	86.46(8)	N(1)−Ni(1)−N(2)	79.05(10)
O(5)−Ni(1)−N(2)	97.65(9)		

Table S3. Selected bond distances and angles for complex **1b**.

Bond distances (Å)			
Ni(1)−N(1)	2.062(2)	C(7)−O(2)	2.259(3)
Ni(1)−O(1)	2.0396(19)	C(7)−O(3)	2.245(4)
Ni(1)−O(2)	2.024(2)	C(10)−O(1)	1.266(3)
Bond angles (º)			
O(1)−Ni(1)−O(1)’	91.37(11)	O(2)’−Ni(1)−O(2)	172.45(10)
O(1)−Ni(1)−N(1)	172.69(8)	O(2)−Ni(1)−N(1)	89.90(9)
O(1)’−Ni(1)−N(1)	94.59(10)	O(2)−Ni(1)−N(1)’	95.90(9)
O(2)−Ni(1)−O(1)	86.01(8)	N(1)−Ni(1)−N(1)’	79.79(14)
O(2)−Ni(1)−O(1)’	86.71(8)		

Table S4. Selected bond distances and angles for complex **1c**.

Bond distances (Å)			
Ni(01)−O(1)	2.045(3)	Ni(01)−N(4)	2.083(4)
Ni(01)−O(2)	2.054(3)	Ni(01)−N(1)	2.079(4)
Ni(01)−N(3)	2.061(4)	C(11)−O(1)	1.302(6)
Ni(01)−N(2)	2.085(4)	C(20)−O(2)	1.285(6)
Bond angles (º)			
O(1)−Ni(01)−O(2)	168.96(13)	N(3)−Ni(01)−N(2)	92.57(15)
O(1)−Ni(01)−N(3)	80.61(14)	N(3)−Ni(01)−N(4)	94.40(15)
O(1)−Ni(01)−N(2)	97.05(15)	N(3)−Ni(01)−N(1)	169.13(16)
O(1)−Ni(01)−N(4)	94.16(15)	N(4)−Ni(01)−N(2)	167.64(15)
O(1)−Ni(01)−N(1)	94.45(15)	N(1)−Ni(01)−N(2)	78.35(16)
O(2)−Ni(01)−N(3)	90.41(14)	N(1)−Ni(01)−N(4)	95.62(16)
O(2)−Ni(01)−N(2)	89.72(14)	C(11)−O(1)−Ni(01)	112.9(3)
O(2)−Ni(01)−N(4)	80.04(14)	C(20)−O(2)−Ni(01)	112.6(3)
O(2)−Ni(01)−N(1)	95.46(15)		

Table S5. Hydrogen bonding interactions in the structures of the complexes **1a-1c**.

D−H···A	D(D···H) **(Å)**	d(H···A) **(Å)**	d(D···A) **(Å)**	<(DHA) **(º)**
1a				
O(8)−H(8A)···O(6)	0.820	1.898	2.708	169.42
O(8)···O(9)			2.936	
1b				
O(4)−H(4B)···O(3)	0.850	1.905	2.737	165.80
O(5)−H(5A)···O(3)	0.849	1.948	2.772	163.23
O(4)−H(4A)···O(5)	0.849	1.933	2.767	167.08
O(3)···O(4)			2.737	
O(6)···O(4)			2.741	
1c				
O(3)−H(3B)···O(2)	0.850	1.877	2.712	166.70
O(3)−H(3A)···O(1)	0.850	1.890	2.740	177.23

Table S6. Protein-binding constant (K_b), number of binding sites per albumins (n) and relative thermodynamic parameters (ΔG^o, ΔS^0 and ΔH^0) of the interaction of Ni^{II} complexes with SAs at different temperatures (25, 30 and 35ºC).

Complexes	T (^0C)	$K_{sv}\times10^4$ ($M^{-1}s^{-1}$)	$K_q\times10^{12}$ (M^{-1})	$K_b\times10^5$ (M^{-1})	n	ΔG^o $kJmol^{-1}$	ΔS^o $Jmol^{-1}$	ΔH^o $kJmol^{-1}$
				BSA				
1a	25	1.55(±0.23)	1.55(±0.23)	5.69(±0.09)	1.39	−32.83		
	30	1.47(±0.20)	1.47(±0.20)	5.58(±0.07)	1.32	−33.33	96.37	−4.13
	35	1.38(±0.22)	1.38(±0.22)	5.39(±0.07)	1.30	−33.79		
1b	25	2.06(±0.25)	2.06(±0.25)	6.26(±0.05)	1.29	−33.06		
	30	1.80(±0.23)	1.80(±0.25)	6.04(±0.02)	1.34	−33.53	57.15	−16.10
	35	1.62(±0.23)	1.62(±0.25)	5.07(±0.06)	1.21	−33.63		
1c	25	2.03(±0.18)	2.03(±0.18)	6.86(±0.10)	1.30	−32.29		
	30	1.48(±0.19)	1.48(±0.19)	6.01(±0.13)	1.43	−33.52	66.72	−13.40
	35	1.08(±0.18)	1.08(±0.18)	5.73(±0.12)	1.21	−33.95		
				HSA				
1a	25	2.22(±0.15)	2.22(±0.15)	5.85(±0.03)	1.40	−32.90		
	30	1.88(±0.17)	1.88(±0.17)	5.82(±0.06)	1.38	−33.43	102.85	−2.26
	35	1.31(±0.15)	1.31(±0.15)	5.68(±0.05)	1.18	−33.92		
1b	25	3.66(±0.21)	3.66(±0.21)	6.66(±0.10)	1.46	−33.22		
	30	2.89(±0.10)	2.89(±0.10)	4.79(±0.19)	1.13	−32.94	7.457	−35.40
	35	2.16(±0.18)	2.16(±0.18)	4.14(±0.16)	1.02	−33.11		
1c	25	1.27(±0.10)	1.27(±0.10)	5.77(±0.02)	1.25	−32.86		
	30	0.86(±0.12)	0.86(±0.12)	4.93(±0.04)	0.97	−33.02	10.21	−29.90
	35	0.57(±0.12)	0.57(±0.12)	3.89(±0.06)	1.01	−32.95		

Table S7. The proteins binding constant (K_b) values for Ni^{II} complexes reported.

Complexes	K_b		**References**
	BSA	**HSA**	
$[Ni(nal)_2(bpy)]$	$5.69(\pm0.09)\times10^5$	$5.85(\pm0.03)\times10^5$	**This Work**
$[Ni(nal)_2(phen)]$	$6.26(\pm0.05)\times10^5$	$6.66(\pm0.10)\times10^5$	
$[Ni(8\text{-}Hq)_2(bpy)]$	$6.86(\pm0.10)\times10^5$	$5.77(\pm0.02)\times10^5$	
nal = Nalidixic Acid, bpy = 2,2'-bipyridine, phen = 1,10-phenanhroline, 8-Hq = 8-Hydroxyquinolone			
$[Ni(erx)_2(H_2O]$	$5.64(\pm0.10)\times10^4$	$5.68(\pm0.42)\times10^4$	
$[Ni(erx)_2(phen)]$	$1.12(\pm0.08)\times10^5$	$3.30(\pm0.28)\times10^4$	18
$[Ni(erx)_2(bpy)]$	$1.03(\pm0.07)\times10^5$	$8.83(\pm0.74)\times10^4$	
$[Ni(erx)_2(py)_2]$	$7.51(\pm0.25)\times10^4$	$9.43(\pm0.45)\times10^4$	
erx = Enrofloxacin, py = Pyridine			
$[Ni(nap)_2(MeOH)_4]$	$4.51(\pm0.34)\times10^4$	$1.35(\pm0.11)\times10^4$	
$[Ni(nap)_2(bpy)(CH_3OH)]$	$3.25(\pm0.31)\times10^5$	$1.93(\pm0.03)\times10^5$	
$[Ni(nap)_2(phen)(H_2O)]$	$4.18(\pm0.34)\times10^5$	$2.73(\pm0.25)\times10^4$	19
$[Ni(nap)_2(bipyam)_2]$	$4.59(\pm0.35)\times10^4$	$1.88(\pm0.26)\times10^5$	
$[Ni(nap)_2(Hpko)_2]$	$1.08(\pm0.07)\times10^5$	$3.02(\pm0.41)\times10^4$	
$[Ni(erx)_2(py)_2(H_2O)_2]$	$7.44(\pm0.55)\times10^3$	$4.05(\pm0.23)\times10^4$	
Hnap = Naproxen, bipyam = 2,2'-dipyridylamine, Hpko = 2,2'-dipyridylketone oxime			
$[Ni(mef)_2(bpy)(MeOH)_2]$	$3.23(\pm0.14)\times10^5$	$2.44(\pm0.08)\times10^5$	
$[Ni(mef)_2(phen)(MeOH)_2]$	$3.10(\pm0.14)\times10^5$	$2.23(\pm0.14)\times10^5$	
$[Ni(mef)_2(bipyam)_2]$	$2.33(\pm0.11)\times10^5$	$2.03(\pm0.16)\times10^5$	20
$[Ni(mef)_2(Hpko)_2]$	$1.35(\pm0.07)\times10^5$	$3.42(\pm0.23)\times10^5$	
$[Ni(mef)_2(py)_2(H_2O)_2]$	$3.22(\pm0.09)\times10^5$	$3.85(\pm0.20)\times10^5$	
$[Ni(mef)_2(MeOH)_4]$	$2.11(\pm0.10)\times10^5$	$3.00(\pm0.20)\times10^5$	
Hmef = Mefenamic acid			
$[Ni(dicl)(Hdicl)(Hpko)_2]$	$2.21(\pm0.23)\times10^5$	$2.54(\pm0.27)\times10^4$	
$[Ni(dicl)_2(bpy)]$	$1.31(\pm0.11)\times10^6$	$3.60(\pm0.41)\times10^5$	21
$[Ni(dicl)_2(phen)]$	$1.72(\pm0.13)\times10^5$	$6.87(\pm0.42)\times10^5$	
Nadicl = Sodium diclofenac			
$[Ni(indo)_2(MeOH)_4]$	$1.59(\pm0.07)\times10^5$	$7.55(\pm0.07)\times10^4$	
$[Ni(indo)(bipyam)_2]Cl$	$1.03(\pm0.03)\times10^5$	$8.00(\pm0.07)\times10^4$	
$[Ni(indo)_2(bpy)(MeOH)_2]$	$4.24(\pm0.02)\times10^4$	$4.72(\pm0.07)\times10^4$	
$[Ni(indo)_2(bipyam)]$	$1.48(\pm0.07)\times10^5$	$1.59(\pm0.07)\times10^4$	22
$[Ni(indo)_2(phen)(MeOH)_2]$	$5.14(\pm0.03)\times10^4$	$6.30(\pm0.07)\times10^4$	
$[Ni(indo)_2(Hpko)_2]$	$1.70(\pm0.06)\times10^5$	$3.73(\pm0.07)\times10^4$	
indo = Indomethacin			
$[Ni(tolf)_2(H2O)_2]$	$3.76(\pm0.35)\times10^5$	$1.59(\pm0.15)\times10^5$	
$[Ni(tolf)_2(bpy)(MeOH)_2]$	$3.73(\pm0.38)\times10^5$	$2.23(\pm0.11)\times10^5$	
$[Ni(tolf)_2(phen)(MeOH)_2]$	$4.92(\pm0.41)\times10^5$	$1.46(\pm0.06)\times10^5$	23
$[Ni(tolf)_2(bipyam]$	$4.86(\pm0.34)\times10^5$	$1.32(\pm0.04)\times10^5$	
$[Ni(tolf)_2(Hpko)_2]$	$3.12(\pm0.29)\times10^5$	$2.08(\pm0.10)\times10^5$	
$[Ni(tolf)_2(py)_2(MeOH)_2]$	$1.57(\pm0.14)\times10^5$	$1.44(\pm0.09)\times10^5$	
tolf = Tolfenamic acid			
$[Ni(difl)_2(MeOH)_4]$	$1.69(\pm0.09)\times10^5$	$1.41(\pm0.08)\times10^5$	24
$[Ni(difl)_2(Hpko)_2]$	$9.78(\pm0.82)\times10^4$	$1.25(\pm0.06)\times10^5$	
$[Ni(difl)_2(phen)(MeOH)_2]$	$9.70(\pm0.66)\times10^4$	$2.68(\pm0.20)\times10^5$	
$[Ni(difl)_2(bpy)(MeOH)]$	$7.33(\pm0.34)\times10^4$	$2.66(\pm0.17)\times10^5$	

[Ni(difl)$_2$(bipyam)]	1.04(±0.05)×10^5	1.60(±0.06)×10^5

Table S8. The binding parameters [% hypochromism (Δε), DNA binding constants (K_b), Gibbs free energy (ΔG^o,), Stern–Volmer constant (K_{SV}) and apparent binding constant (K_{app})] of complexes **1a**-**1c**.

Complexes	Δε (%)	K_b×10^5 (M^{-1})	ΔG^o, (kJ mol^{-1})	K_{SV}×10^5 (M^{-1})	K_{app}×10^6 (M^{-1})
1a	33% (band I), 26% (band II)	2.81(±0.08)	−32.00	1.14(±0.10)	2.50
1b	32% (band I), 11% (band II)	5.51(±0.07)	−33.42	0.83(±0.15)	2.85
1c	21% (band I), 16% (band II), 15% (band III), 12% (band IV)	4.31(±0.03)	−37.39	1.51(±0.12)	4.0

Table S9. DNA-binding constant (K_b) and Stern-Volmer quenching constant (K_{SV}) values for nickel complexes reported.

Complexes	K_b	K_{SV}	**References**
[Ni(nal)$_2$(bpy)]	2.81(±0.08)×10^5	1.14(±0.10)×10^5	
[Ni(nal)$_2$(phen)]	5.51(±0.07)×10^5	0.83(±0.15)×10^5	**This Work**
[Ni(8-Hq)$_2$(bpy)]	4.31(±0.03)×10^5	1.51(±0.12)×10^5	
nal = Nalidixic Acid, bpy = 2,2'-bipyridine, phen = 1,10-phenanhroline, 8-Hq = 8-Hydroxyquinolone			
[Ni(erx)$_2$(H$_2$O)$_2$]	1.75(±0.40)×10^4		18
[Ni(erx)$_2$(bpy)]	1.63(±0.25)×10^4		
[Ni(erx)$_2$(phen)]	4.09(±0.53)×10^4		
[Ni(erx)$_2$(py)$_2$]	2.59(±0.48)×10^5		
erx = Enrofloxacin, py = Pyridine			
[Ni(nap)$_2$(MeOH)]	1.47(±0.05)×10^5	1.52(±0.04)×10^5	19
[Ni(nap)$_2$(bpy)(CH$_3$OH]	5.96(±0.10)×10^5	1.29(±0.03)×10^5	
[Ni(nap)$_2$(phen)(H$_2$O)]	1.54(±0.12)×10^5	1.06(±0.04)×10^5	
[Ni(nap)$_2$(bipyam)]	2.91(±0.31)×10^5	9.80(±0.20)×10^4	
Hnap = Naproxen, bipyam = 2,2'-dipyridylamine			
[Ni(mef)$_2$(bpy)(MeOH)$_2$]	1.20(±0.23)×10^5		20
[Ni(mef)$_2$(phen)(MeOH)$_2$]	8.26(±0.19)×10^4		
[Ni(mef)$_2$(bipyam)$_2$]	1.46(±0.33)×10^5		
[Ni(mef)$_2$(py)$_2$(H$_2$O)$_2$]	1.19(±0.25)×10^5		
[Ni(mef)$_2$(MeOH)$_4$]	2.62(±0.35)×10^5		
Hmef = Mefenamic acid			
[Ni(dicl)(Hdicl)(Hpko)$_2$]	3.63(±0.12)×10^5		21
[Ni(dicl)$_2$(bpy)]	2.21(±0.08)×10^5		
[Ni(dicl)$_2$(phen)]	3.67(±0.17)×10^4		
Nadicl = Sodium diclofenac			
[Ni(indo)$_2$(MeOH)$_4$]	2.09(±0.02)×10^5	1.24(±0.03)×10^5	22

$[Ni(indo)(bipyam)_2]Cl$	$4.42(\pm0.15)\times10^4$		
$[Ni(indo)_2(bpy)(MeOH)_2]$	$2.32(\pm0.06)\times10^5$		
$[Ni(indo)_2(bipyam)]$	$4.75(\pm0.25)\times10^5$	$1.47(\pm0.04)\times10^5$	
$[Ni(indo)_2(Hpko)_2]$	$4.15(\pm0.27)\times10^5$		
$[Ni(tolf)_2(H_2O)_4]$	$9.50(\pm0.25)\times10^4$	$7.95(\pm0.03)\times10^4$	23
$[Ni(tolf)_2(bpy)(MeOH)_2]$	$2.35(\pm0.12)\times10^5$		
$[Ni(tolf)_2(Hpko)_2]$	$2.80(\pm0.35)\times10^5$		
Htolf = tolfenamic acid, bpy = 2,2'-bipyridine, Hpko = 2,2'-dipyridylketone oxime			
$[Ni(difl)_2(MeOH)$	$2.00(\pm0.17)\times10^5$	$8.26(\pm0.22)\times10^4$	24
$[Ni(difl)_2(phen)(MeOH)$	$8.35(\pm0.05)\times10^4$	$9.27(\pm0.59)\times10^4$	
$[Ni(difl)_2(bipyam)]$	$2.00(\pm0.20)\times10^5$	$9.56(\pm0.45)\times10^4$	
$Ni\mathbf{L^2}$	2.0×10^4		25
$Ni\mathbf{L^3}$	1.0×10^4		
$\mathbf{L^2}$ = (E)-3-hydroxy-N'-(1-(pyrazin-2-yl)ethylidene)benzohydrazide, $\mathbf{L^3}$ = (E)-4-hydroxy-N'-(1-(pyrazin-2-yl)ethylidene)benzohydrazide			
$[Ni(\eta\text{-}NO_3)(bta)(phen)]$	6.05×10^3		26
$[Ni(\eta\text{-}NO_3)(btc)(phen)]$	1.31×10^4		
$[Ni(\eta\text{-}NO_3)(btf)(phen)]$	4.94×10^4		
bta = 4,4,4-trifluoro-1-phenyl-1,3-butanedione anion, btc = 1-(4-chlorophenyl)-4,4,4-trifluoro-1,3-butanedione anion, btf = 4,4,4-trifluoro-1-(2-furyl)-1,3-butanedione anion, phen = 1,10-phenanthroline			
$[Ni(phen)_3]$	$1.40(\pm0.16)\times10^4$		27
$[Ni(5,6\text{-}dmp)_3]$	$3.17(\pm0.07)\times10^4$		
$[Ni(dpq)_2]$	$5.80(\pm0.10)\times10^4$		
$[Ni_2\mathbf{L^1}]$	1.17×10^4	1.02	28
$[Ni_2\mathbf{L^2}]$	2.0×10^4	1.11	
$[Ni_2\mathbf{L^3}]$	2.0×10^4	1.06	
$[Ni_2\mathbf{L^4}]$	5.0×10^4	2.92	
$[Ni_2\mathbf{L^5}]$	1.16×10^5	3.6	
$\mathbf{L^1}$ =1,2-diamino ethane, $\mathbf{L^2}$ = 1,3-diamino propane, $\mathbf{L^3}$ = 1,4-diamino butane, $\mathbf{L^4}$ = 1,2-diamino benzene and $\mathbf{L^5}$ = 1,8-diamino naphthalene			
$[Ni(\mathbf{L^1})_2]$	$1.14(\pm0.05)\times10^5$	$1.13(\pm0.04)\times10^5$	29
$[Ni(\mathbf{L^2})_2]$	$0.98(\pm0.10)\times10^5$	$1.02(\pm0.12)\times10^5$	
$[Ni(\mathbf{L^3})_2]$	$0.97(\pm0.08)\times10^5$	$1.01(\pm0.18)\times10^5$	
$[Ni(\mathbf{L^4})_2]$	$0.89(\pm0.06)\times10^5$	$1.00(\pm0.28)\times10^5$	
$\mathbf{L^1}$ = N-(2-Methylphenyl)pyridine-2-thiocarboxamide, $\mathbf{L^2}$ = N-(4-Methylphenyl)pyridine-2-thiocarboxamide, $\mathbf{L^3}$ = N-(2,4,6-Trimethylphenyl)pyridine-2-thiocarboxamide, $\mathbf{L^4}$ = N-(2-Chlorophenyl)pyridine-2-thiocarboxamide			
$NiL_2phen.CH_3CN$	$1.20(\pm0.15)\times10^5$	$4.45(\pm0.06)\times10^4$	30
$[Ni(\mathbf{L^1})_2]$	1.50×10^4	1.30×10^4	31
$[Ni(\mathbf{L^2})_2]$	3.74×10^4	1.50×10^4	
$[Ni(\mathbf{L^3})_2]$	4.02×10^4	4.02×10^4	
$[Ni(\mathbf{L^4})_2]$	8.56×10^4	8.56×10^4	
$[Ni(\mathbf{L^5})_2]Cl_2$	1.35×10^5	1.37×10^5	
L= Schiff bases derived from benzaldehyde			
$[Ni(\mathbf{L^1})_2]$	2.13×10^4		32
$[Ni(\mathbf{L^2})(H\ \mathbf{L^2})].Cl.H_2O$	7.34×10^4		

L^1 = (E)-N-methyl-2-(quinolin-2-ylmethylene)hydrazinecarbothioamide and **L^2** = (E)-N,N-dimethyl-2-(quinolin-2-ylmethylene)hydrazinecarbothioamide			
$[Ni_2(H_2\mathbf{L^1})_2(OAc)_2(C_2H_5OH)_2]_2$	2.39×10^3	1.38	33
$[Ni_4(H\mathbf{L^2})_3(\mu_3\text{-}O)\ (H_2O)_3]$	2.55×10^3	1.52	
H_3L^1 ={2-ethyl-2-((2-hydroxybenzylideneamino)propane-1,3-diol, and **H_3L^2** = 2-ethyl-2-((2-hydroxy-3-methoxybenzylideneamino)propane-1,3-diol			
$[Ni(\mathbf{L^1})_2]$	1.60×10^4	1.47×10^4	34
$[Ni(\mathbf{L^2})_2]$	2.10×10^4	1.80×10^4	
$[Ni(\mathbf{L^3})_2]$	1.63×10^4	1.65×10^4	
$[Ni(\mathbf{L^4})_2]$	2.91×10^4	1.99×10^4	
$[Ni(\mathbf{L^5})_2]$	1.40×10^5	1.27×10^5	
L^1 = (Z)-N-methyl-2-(2-oxoindolin-3-ylidene)hydrazinecarbothioamide, **L^2** = (Z)-2-(1-allyl-2-oxoindolin-3-ylidene)-N-methylhydrazinecarbothioamide, **L^3** = (Z)-N-methyl-2-(1-methyl-2-oxoindolin-3-ylidene)hydrazinecarbothioamide, **L^4** = (Z)-2-(1-benzyl-2-oxoindolin-3-ylidene)-N-methylhydrazinecarbothioamide, **L^5** = (Z)-2-(5-bromo-1-methyl-2-oxoindolin-3-ylidene)-N-methylhydrazinecarbothioamide			

Table S10. Cathodic and Anodic Potentials (in V) for the Redox Couple Ni^{II}/Ni^{I} in ½ DMSO: buffer Solution of the Complexes in the Absence as well as Presence of CT DNA.

Complexes	$E^a_{pc(f)}$	$E^b_{pc(b)}$	ΔE^c_{pc}	$E^a_{pa(f)}$	$E^b_{pa(b)}$	ΔE^c_{pa}
1a	−0.916	−0.875	+0.041	−0.481	−0.419	+0.062
1b	−0.850	−0.818	+0.032	−0.285	−0.248	+0.037
1c	−0.793	−0.757	+0.036	−0.332	−0.277	+0.055

[a] $E_{pc/a}$ in ½ DMSO: buffer solution in the absence of CT DNA solution $E_{pc/a(f)}$.

[b] $E_{pc/a}$ in ½ DMSO: buffer solution in the presence of CT DNA $E_{pc/a(b)}$.

[c] $\Delta E_{pc/a} = E_{pc/a(b)} - E_{pc/a(f)}$.

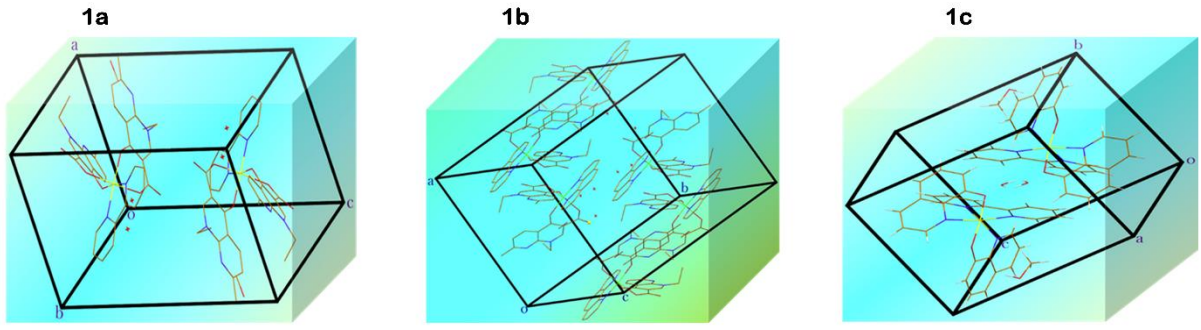

Fig. S1. Crystal packing representations of the complexes **1a**-**1c**.

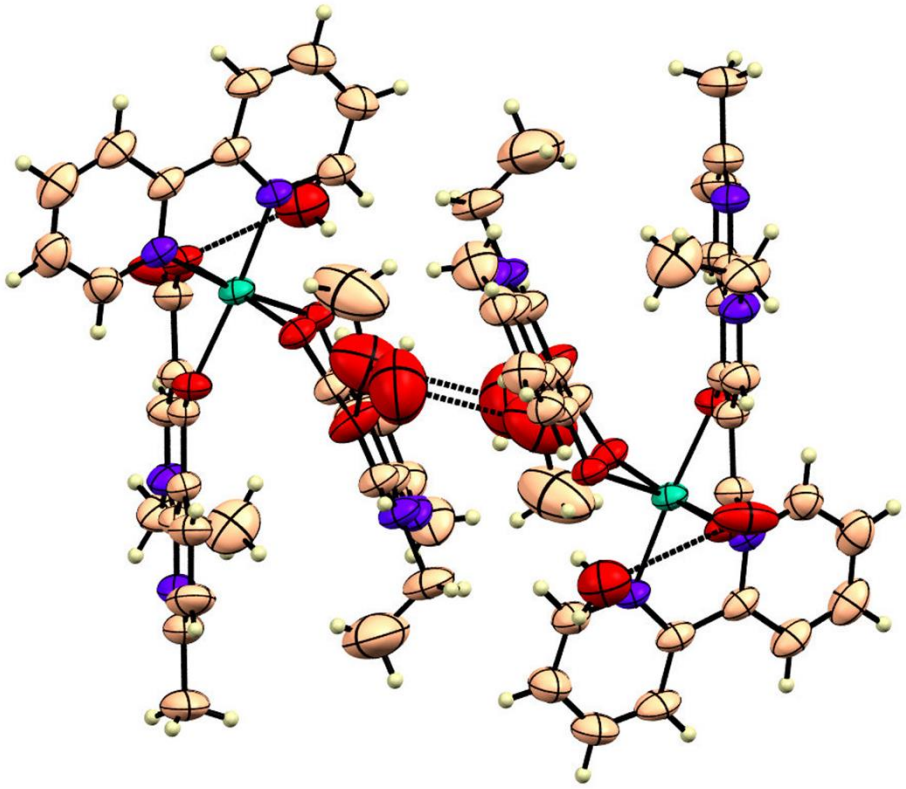

Fig. S2. Intermolecular hydrogen bonding interactions in complex **1a** leading to the formation of cage-like structure.

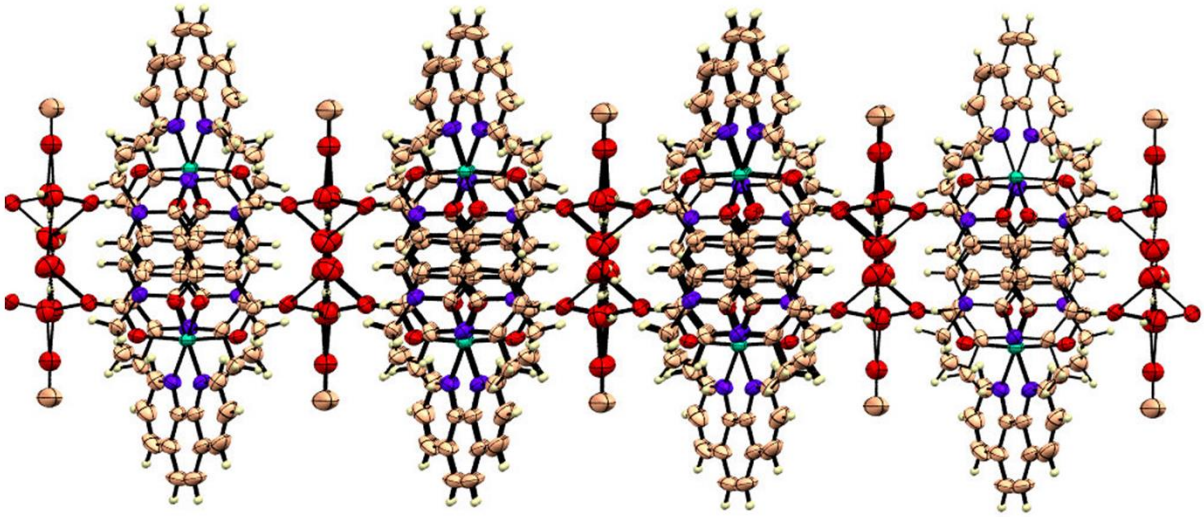

Fig. S3. Intermolecular hydrogen bonding interactions in complex **1b** leading to the formation of chain structure.

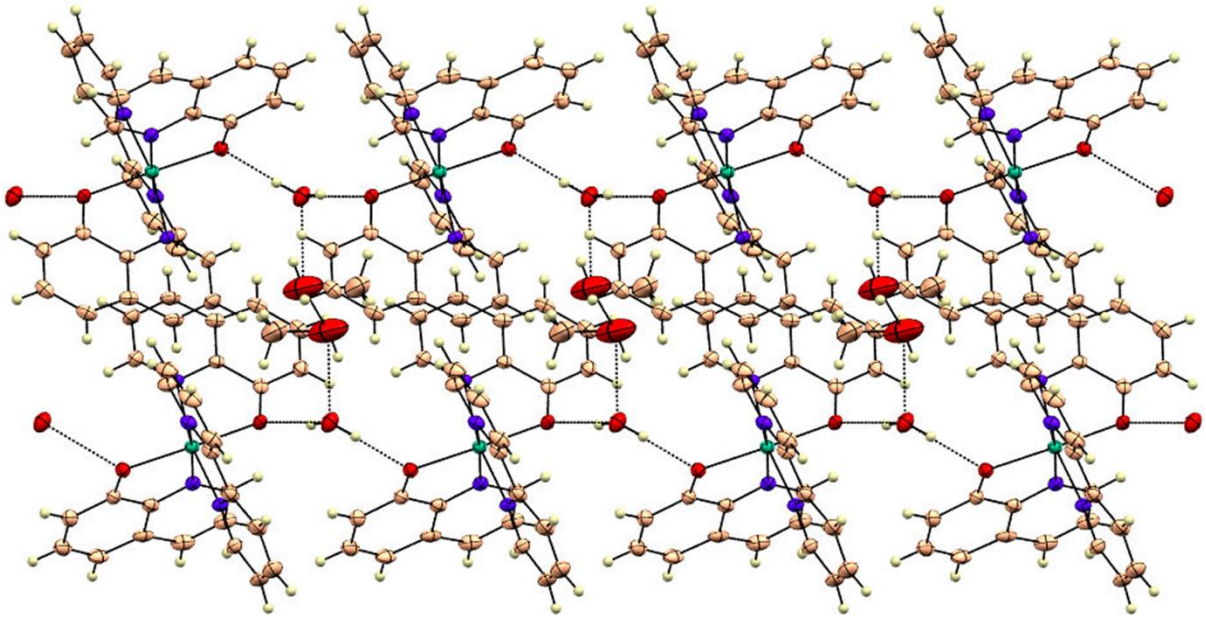

Fig. S4. Intermolecular hydrogen bonding interactions in complex **1c** leading to the formation of cage-like structure.

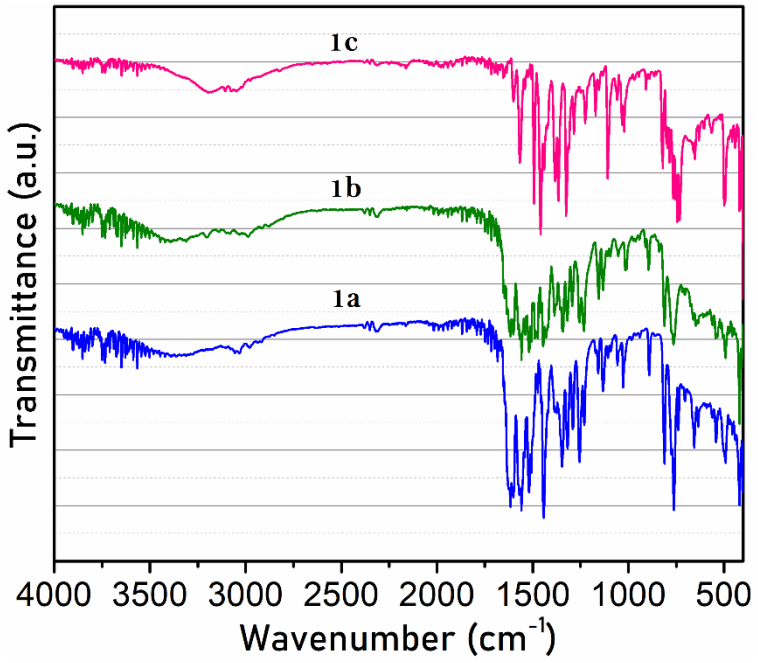

Fig. S5. FT-IR spectrum of complexes **1a-1c**.

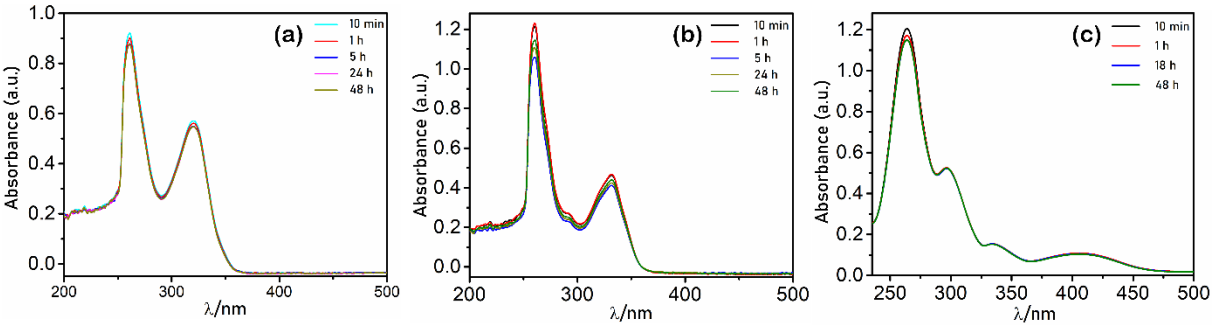

Fig. S6. The stability plots of complexes **(a)** [Ni(nal)$_2$bpy] **1a**, **(b)** [Ni(nal)$_2$phen] **1b** and **(c)** [Ni(8-Hq)$_2$bpy], **1c** in different time periods.

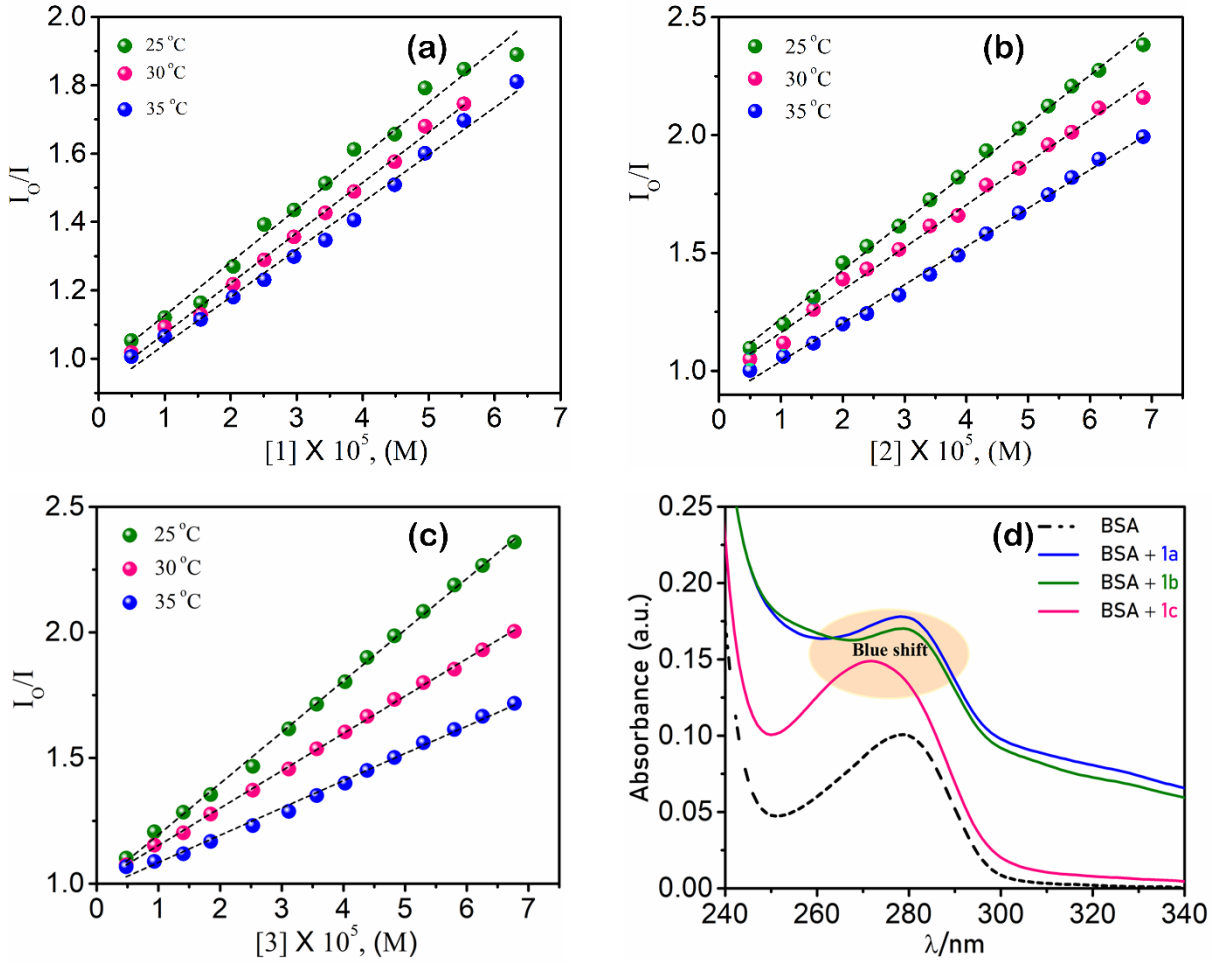

Fig. S7. The Stern-Volmer plots for the quenching of BSA (20 μM) by the complexes **(a) 1a**, **(b) 1b** and **(c) 1c** at three different temperatures (25, 30 and 35ºC). **(d)** UV/Vis absorption spectrum of BSA (black dashed line) in the presence of complexes (other lines).

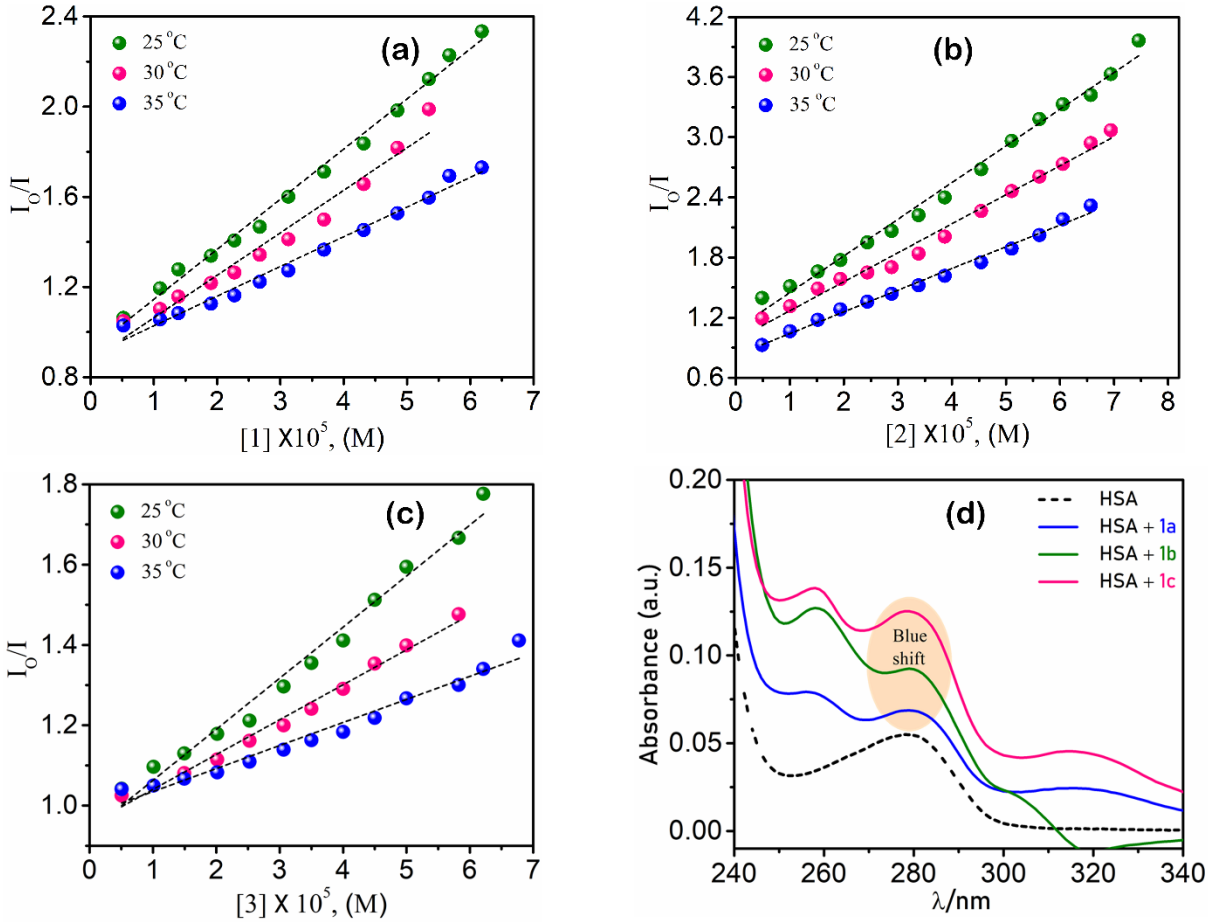

Fig. S8. The Stern-Volmer plots for the quenching of HSA (20 μM) by the complexes **(a) 1a**, **(b) 1b** and **(c) 1c** at three different temperatures (25, 30 and 35ºC). **(d)** UV/Vis absorption spectrum of HSA (black dashed line) in the presence of complexes (other lines).

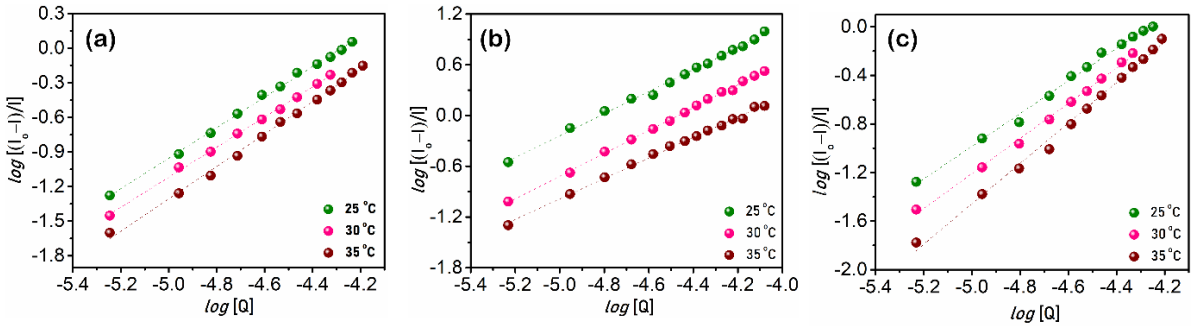

Fig. S9. Scatchard plots of BSA at different temperature for complexes **1a-1c**.

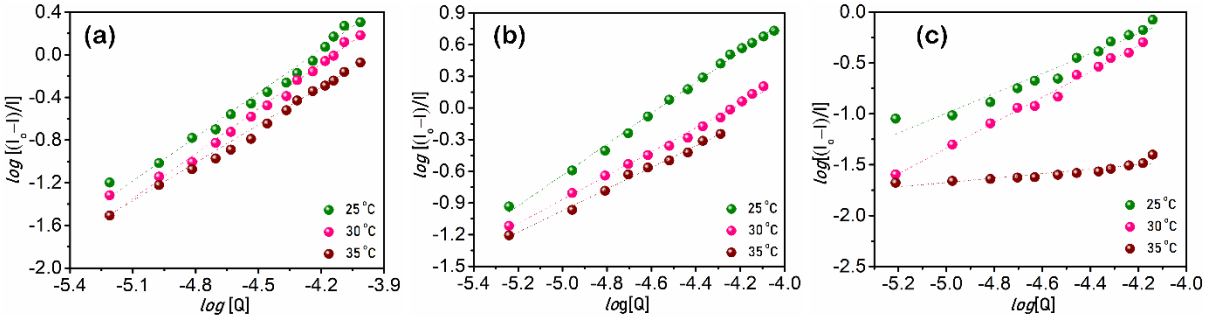

Fig. S10. Scatchard plots of HSA at different temperature for complexes **1a-1c**.

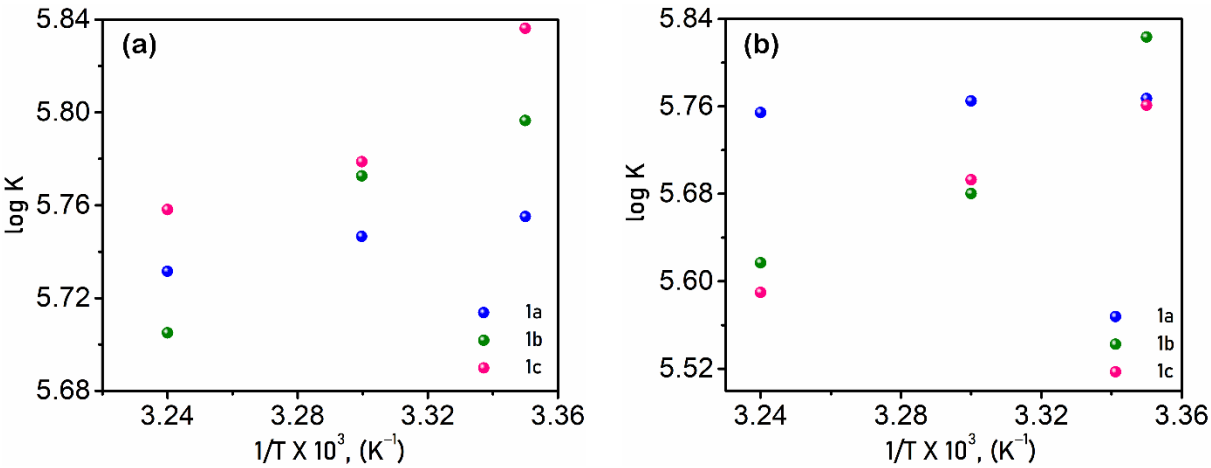

Fig. S11. The van't Hoff graphs for the binding of **(a)** BSA and **(b)** HSA for complexes **1a-1c** at 298, 303, and 308 K (25, 30 and 35ºC).

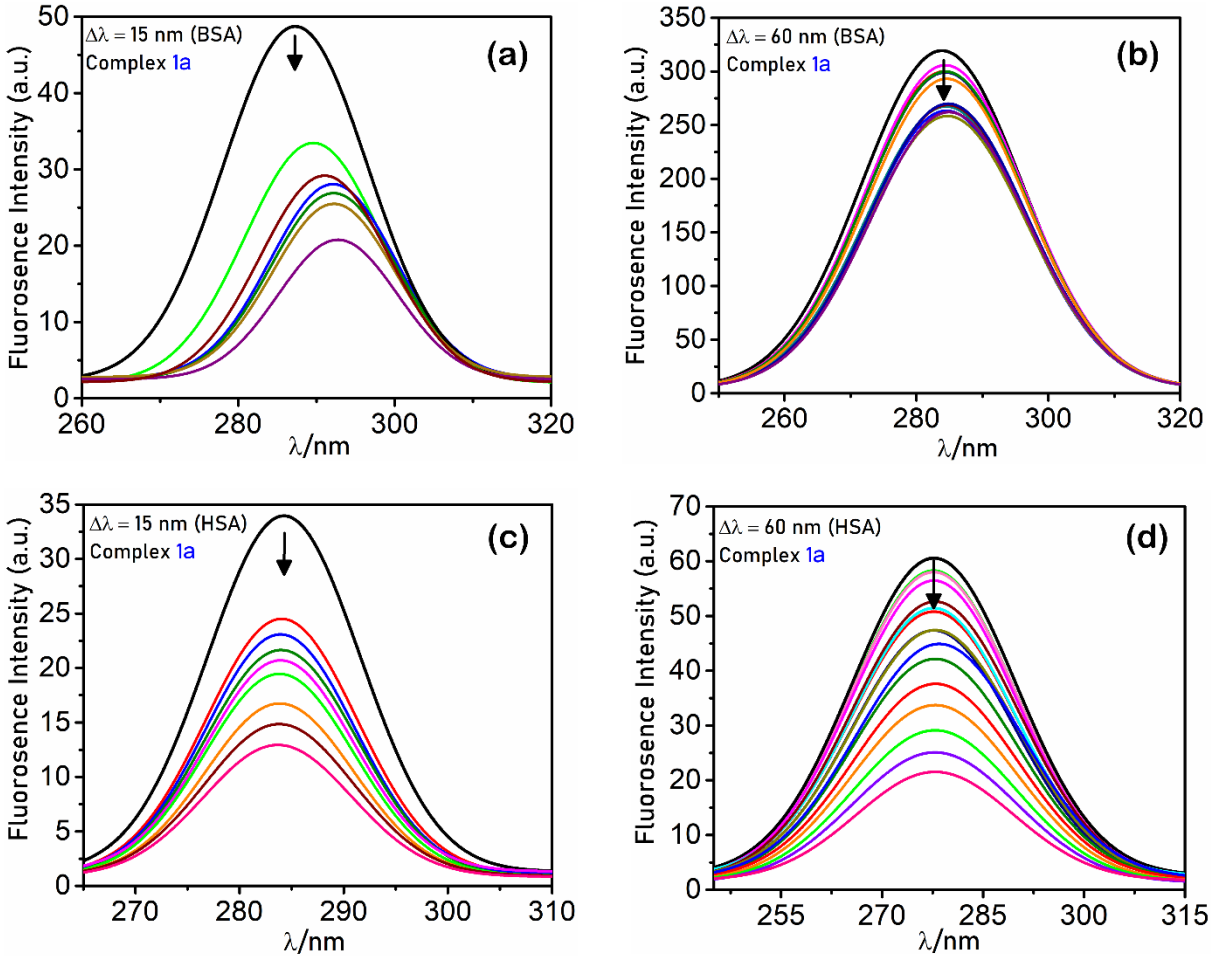

Fig. S12. Synchronous fluorescence spectra of free BSA and HSA in the presence of the increasing concentrations of complexes **1a** at Δλ = 15 and 60 nm. Arrows (↓) show that the intensity changes upon increasing concentrations of the complexes.

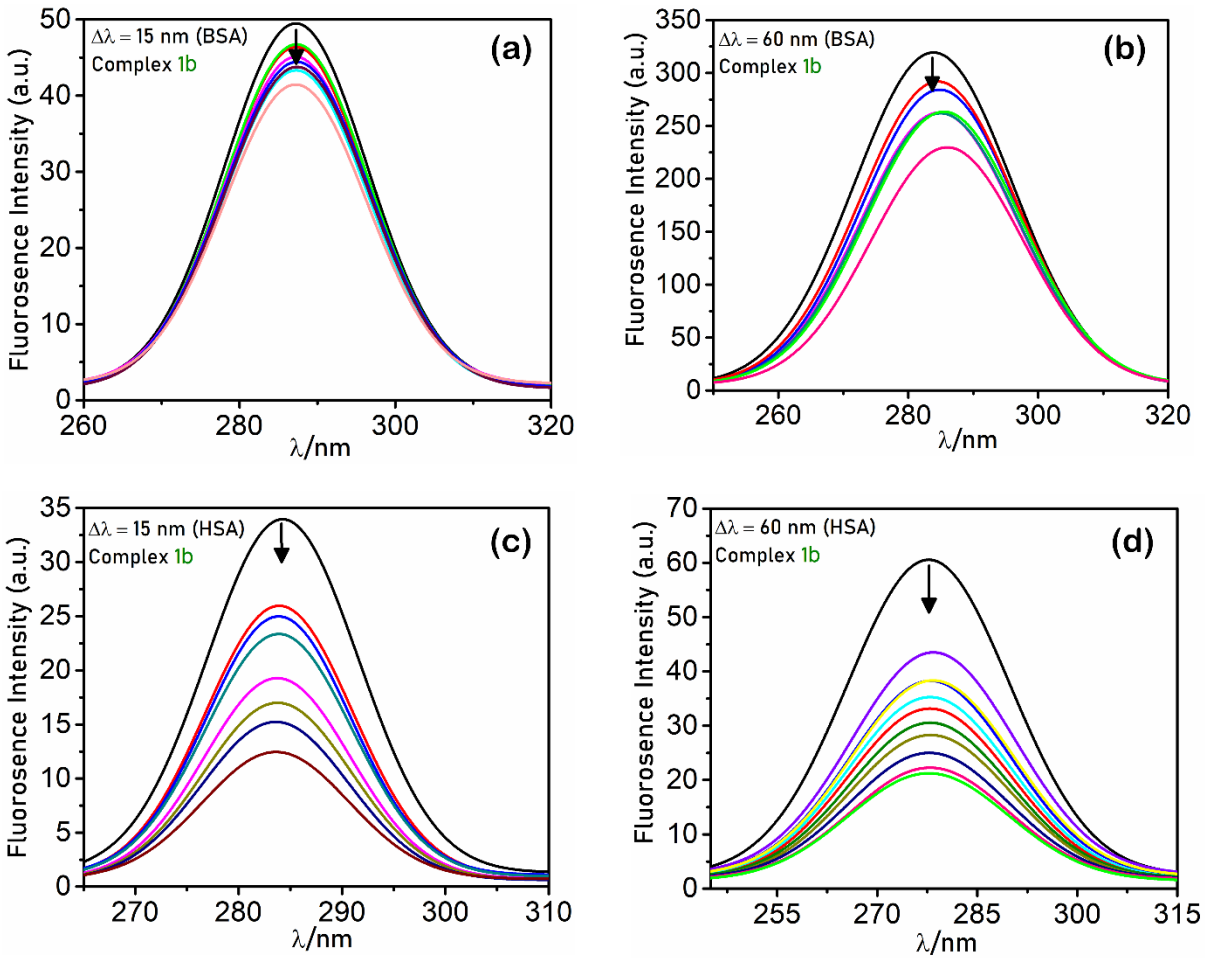

Fig. S13. Synchronous fluorescence spectra of free BSA and HSA in the presence of the increasing concentrations of complexes **1b** at Δλ = 15 and 60 nm. Arrows (↓) show that the intensity changes upon increasing concentrations of the complexes.

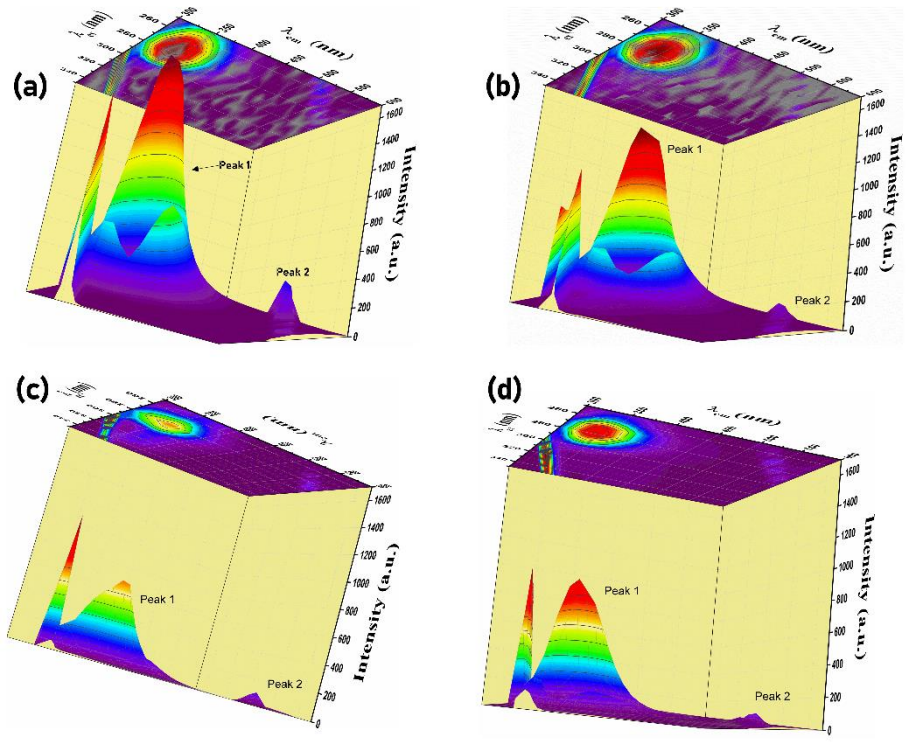

Fig. S14. Three dimensional (3D) fluorescence spectra of **(a)** BSA **(b)** BSA + **1a (c)** BSA + **1b** and **(d)** BSA + **1c**. Concentrations of BSA = 10 μM and **1a-1c** = 10 μM.

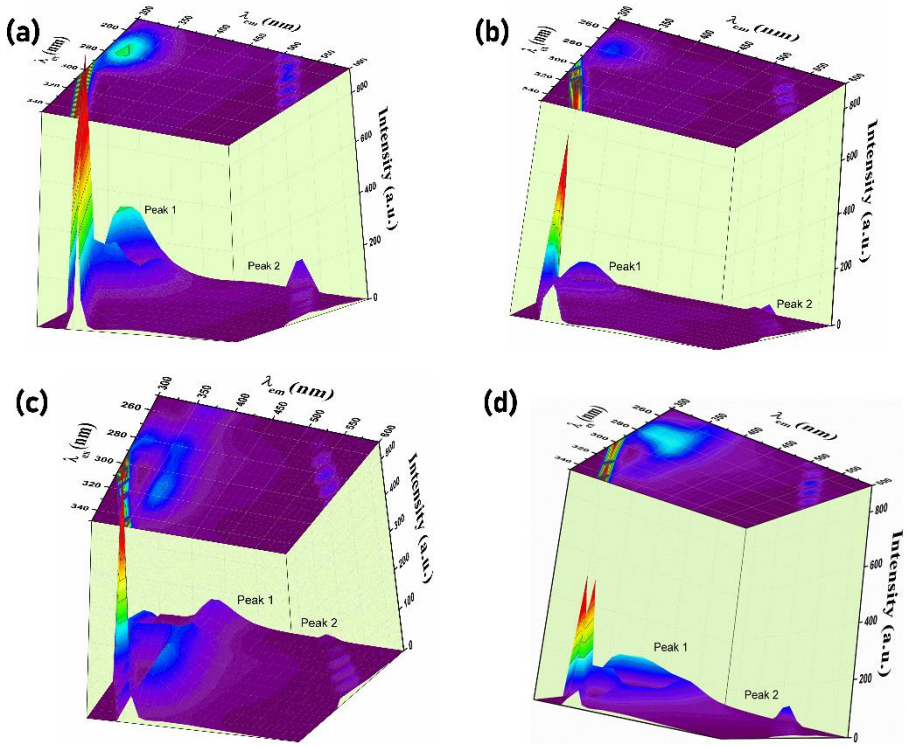

Fig. S15. Three dimensional (3D) fluorescence spectra of **(a)** HSA **(b)** HSA + **1a (c)** HSA + **1b** and **(d)** HSA + **1c**. Concentrations of HSA = 10 μM and **1a-1c** = 10 μM.

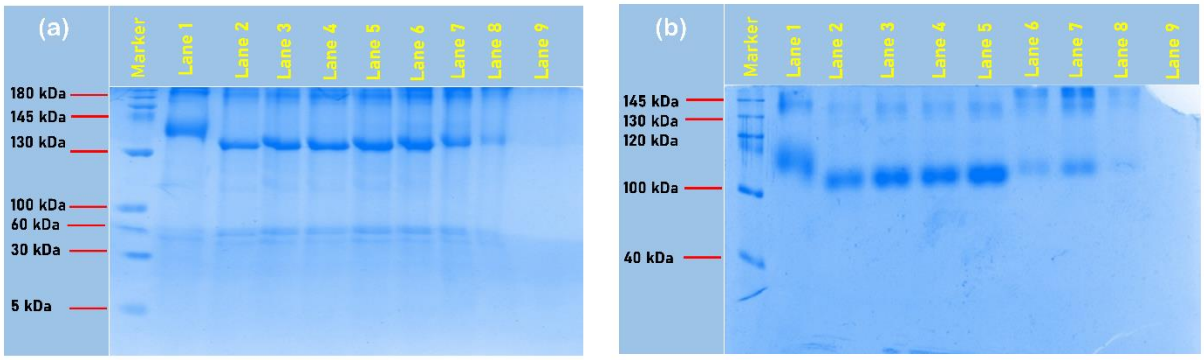

Fig. S16. SDS-PAGE diagram of bovine serum albumin (BSA, 15 μM) and human serum albumin (HSA, 15 μM) incubated with various concentrations of complexes **1c** in the presence of H_2O_2 (100 μM) in buffer solution (150 mM NaCl and 15 mM trisodium citrate at pH 7.2).

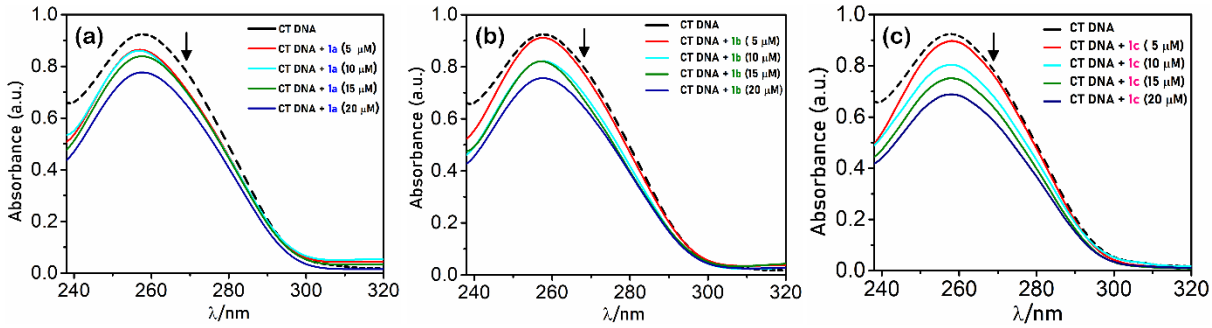

Fig. S17. UV absorbance spectra of CT DNA in a buffer solution containing 150 mM NaCl and 15 mM trisodium citrate at pH 7.4 in the absence as well as the presence of the diverse concentration of complexes **(a) 1a**, **(b) 1b** and **(c) 1c**. The arrows (↓) illustrations the changes occur upon the addition of increasing amounts of complexes.

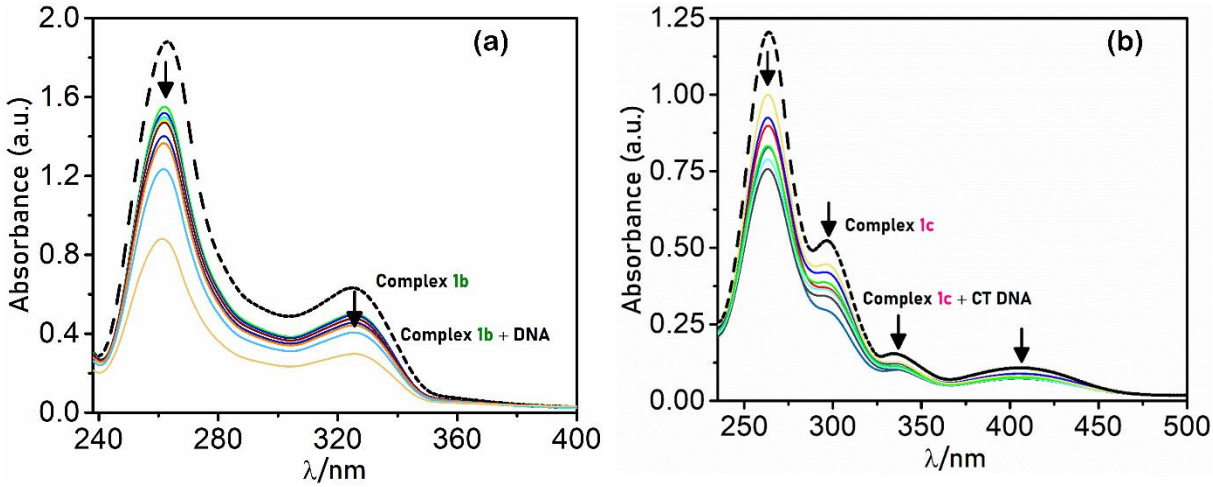

Fig. S18. Absorption spectra of complexes **(a) 1b** and **(c) 1c** upon the titration of CT DNA in 5 mM trisodium citrate/150 mM NaCl buffer. The arrows (↓) display the decreases in absorbance with respect to an increase in the concentration of CT DNA solution (in all).

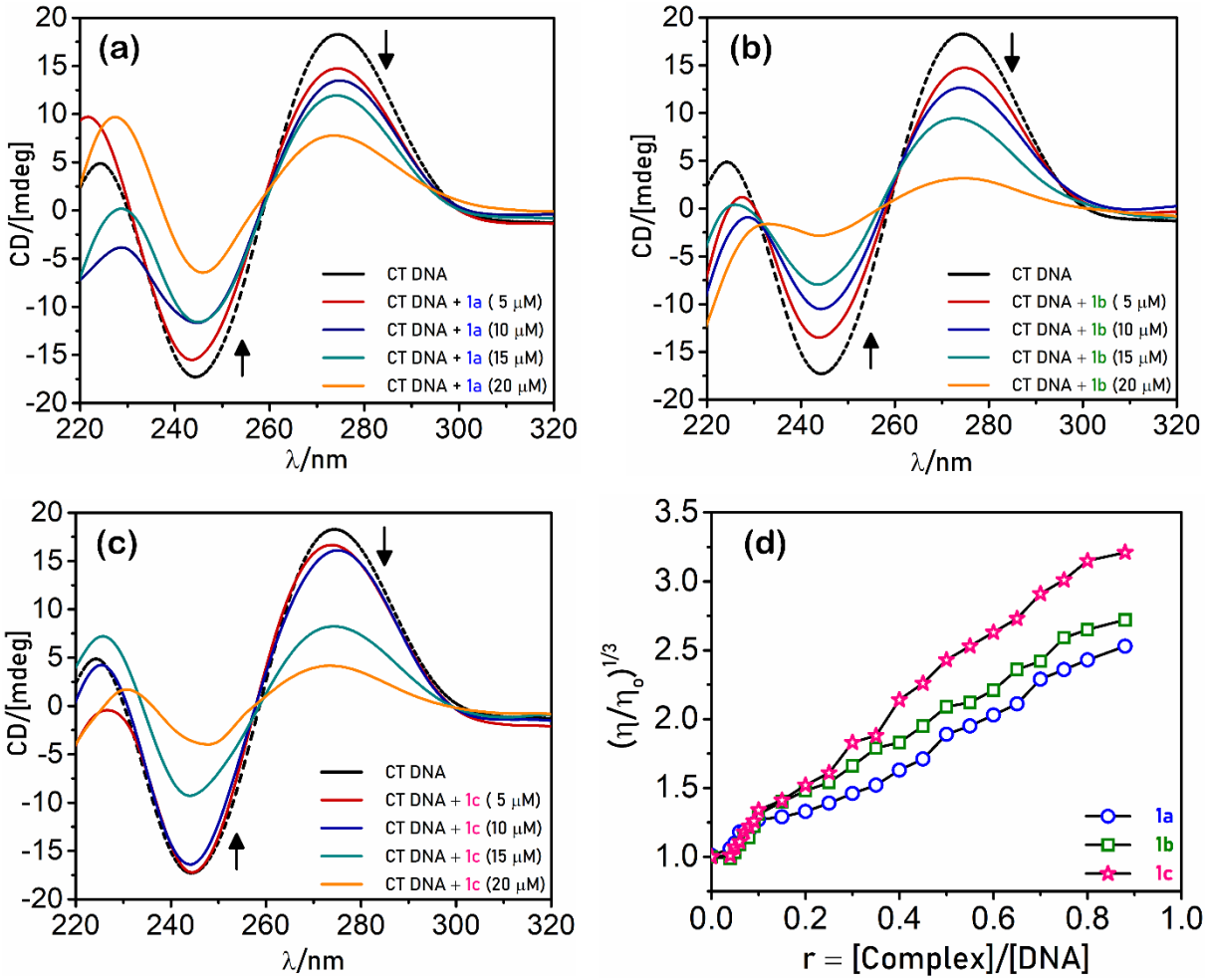

Fig. S19. CD spectrum of free CT DNA solution (black dashed lines) or in the presence of the increasing concentration of complexes **(a) 1a**, **(b) 1b** and **(c) 1c** (other solid lines). **(d)** The effect of the increasing concentration of complexes **1a** (blue line), **1b** (green line), and **1c** (pink line) on the relative viscosity $(\eta/\eta_o)^{1/3}$ of CT DNA at room temperature.

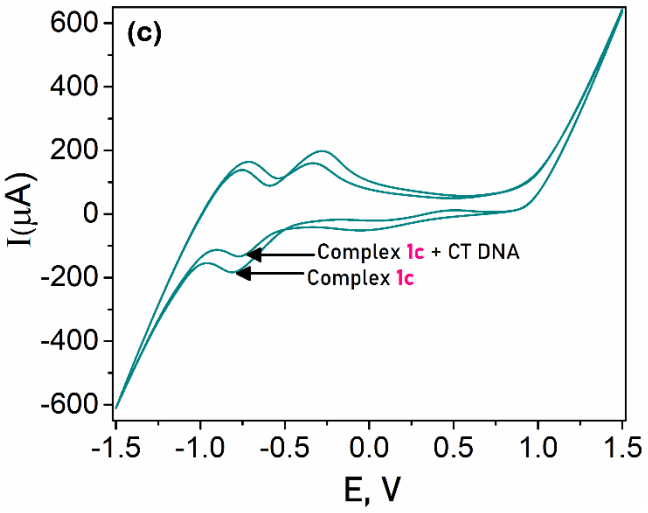

Fig. S20. Cyclic voltammogram of 0.5 mM ½ DMSO: buffer Solution of complex **1c** in the absence as well as in the presence of CT DNA solution. Scan rate = 100 mVs^{-1} (Supporting electrolyte = buffer solution).

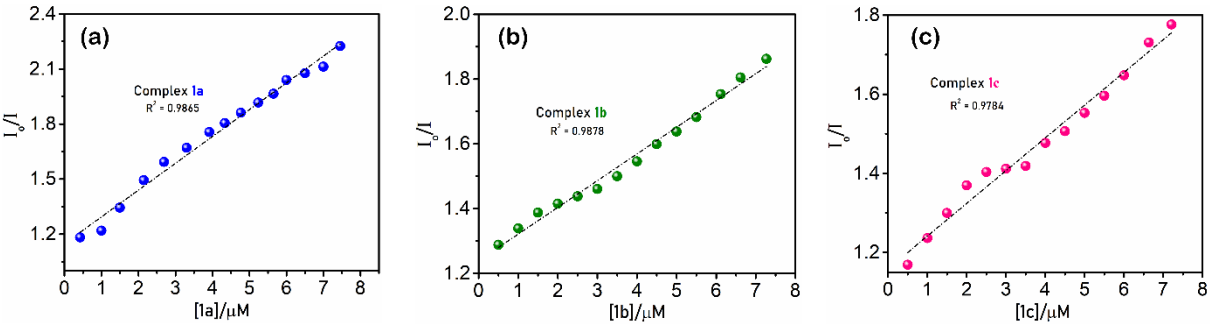

Fig. S21. Stern-Volmer quenching plots of EtBr bound to CT DNA for complexes **1a-1c**.

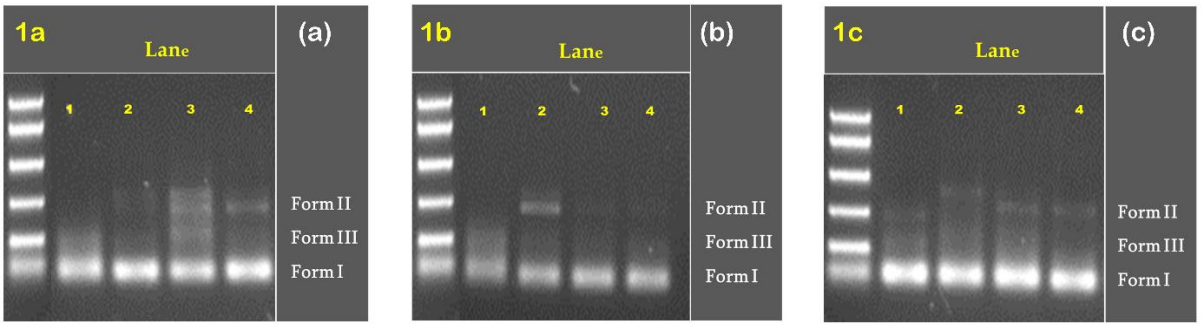

Fig. S22. Gel electrophoresis images of SC plasmid pBR322 DNA incubated with different concentrations of complexes **1a-1c** in the presence of activator-like H_2O_2 for 1 h at 37°C. Form I, II and III represents the supercoiled (SC), nicked circular and linear forms of DNA.

References

(1) CrysAlisPro, version 1.171.33.49b, Oxford Diffraction Ltd, Abingdon, UK, 2009.

(2) O. V. Dolomanov, L. J. Bourhis, R. J. Gildea, J. A. K. Howard and H. Puschmann, *J. Appl. Crystallogr.*, 2009, **42**, 339–341.

(3) G. M. Sheldrick, 2015, **71**, 3–8.

(4) M. Kumar, G. Kumar, D. T. Masram, *New J. Chem.*, 2020**, 44**, 8595-8613.

(5) M. Blagosklonny, W. S. El-Diery, *Int. J. Cancer*, 1996, **67**, 386−392.

(6) E. Ramachandran, D. S. Raja, N. P. Rath, K. Natarajan, *Inorg. Chem.*, 2013, **52**, 1504−1514.

(7) M. Mohanraj, G. Ayyannan, G. Raja, C. Jayabalakrishnan, *Mater. Sci. Eng. C.*, 2016, **69**, 1297−1306.

(8) K. C. Skyrianou, V. Psycharis, C. P. Raptopoulou, D. P. Kessissoglou and G. Psomas, *J. Inorg. Biochem.*, 2011, **105**, 63−74.

(9) E. S. Koumousi, M. Zampakou, C. P. Raptopoulou, V. Psycharis, C. M. Beavers, S. J. Teat, G. Psomas, T. C. Stamatatos, *Inorg. Chem.*, 2012, **51**, 7699−7710.

(10) E. Ramachandran, D. S. Raja, N. P. Rath and K. Natarajan, *Inorg. Chem*., 2013, **52**, 1504−1514.
(11) Y. Manojkumar, S. Ambika, R. Arulkumar, G. Balakrishnan, P. Balaji, G. Vignesh, S. Arunachalam, P. Venuvanalingam, R. Thirumurugan and M. A. Akbarsha, *New. J. Chem*., 2019, **43**, 11391−11407.
(12) M. Kumar, G. Kumar, K. M. Dadure, D. T. Masram, *New. J. Chem*., 2019, **43**, 15462−15481.
(13) J. N. Miller, *Proc. Anal. Div. Chem. Soc*., 1979, **16**, 203−208.
(14) V. D. Suryawanshi, L. S. Waleker, A. H. Gore, V. Anbhule and G. B. Kolekar, *J. Pharm. Anal*., 2016, **6**, 56−63.
(15) C.-L. Zhang, Y.-X. Liu, X.-M. Zhang, S. Chen, F. Shen, Y.-H. Xiong, W. Liu, Z.-W. Mao, X.-Y. Le, *Mater. Sci. Eng. C*., 2018, **91**, 414−425.
(16) P. Vijayan, P. Viswanathamurthi, K. Velmurugan, R. Nandhakumar, M. D. Balakumaran, P. T. Kalaichelvan and J. G. Malecki, *RSC Adv*., 2015, **5**, 103321−103342.
(17) R. K. Gupta, G. Sharma, R. Pandey, A. Kumar, B. Koch, P.-Z. Li, Q. Xu, D. S. Pandey, *Inorg. Chem*., 2013, **52**, 13984−13996.
(18) K. C. Skyrianou, V. Psycharis, C. P. Raptopoulou, D. P. Kessissoglou and G. Psomas, *J. Inorg. Biochem*., 2011, **105**, 63−74.
(19) X. Totta, A. G. Hatzidimitriou, A. N. Papadopoulos, G. Psomas, *New J. Chem*., 2017, **41**, 4478−4492.
(20) X. Totta, A. A. Papadopoulos, A. G. Hatzidimitriou, A. Papadopoulos and G. Psomas, *J. Inorg. Biochem*., **2015**, *145*, 79−93.
(21) M. Kyropoulou, C. P. Raptopoulou, V. Psycharis and G. Psomas, *Polyhedron*, 2013, **61**, 126−136.
(22) S. Perontsis, A. Tialiou, A. N. Hatzidimitriou, A. N. Papadopoulos and G. Psomas, *Polyhedron*, 2017, **138**, 258−269.
(23) X. Totta, A. G. Hatzidimitriou, A. N. Papadopoulos and G. Psomas, *Polyhedron*, 2016, **117**, 172−183.
(24) S. Perontsis, A. G. Hatzidimitriou, A. N. Papadopoulos, G. Psomas, *J. Inorg. Biochem*., 2016, **162**, 9−21.
(25) P. Yang, L.-L. Zhang, Z.-Z. Wang, D.-D. Zhang, Y.-M. Liu, Q.-S. Shi and X.-B. Xie, *J. Inorg. Biochem*., 2020, **203**, 110919.
(26) L. M. Sousa, W. A. Souza, D. A. Paixao, R. B. Fazzi, D. Y. Tezuka, C. D. Lopes, Z. A. Carneiro, M. B. Moreira, M. Pivatto, A. V. G. Netto, Sergio de Albuquerque, F. B. Ferreira, R. J. De Oliveira, A. L. C. Resende, R. C. Lino, R. J. De Oliveira Junior, A. M. Da Costa Ferreira and W. Guerra, *Inorg. Chim. Acta*, 2020, **511**, 119824.
(27) S. Ramakrishnan, E. Suresh, A. Riyasdeen, M. A. Akbarsha and M. Palaniandavar, *Dalton Trans*., 2011, **40**, 3245.
(28) S. Poornima, K. Gunasekaran and M. Kandaswamy, *Dalton Trans*., 2015, **44**, 16361−16371.
(29) R. R. Kumar, M. K. M. Subarkhan and R. Ramesh, *RSC Adv*., 2015, **5**, 46760−46773.

(30) Y. Li, Z. Yang, M. Zhou and Y. Li, *RSC Adv*., 2017, **7**, 49404−49422.
(31) A. Jayamani, S. Nagasubramanian, V. Thamilarasan, S. O. Ojwach and G. Gopu, *Inorg. Chim. Acta*, 2018, **482**, 791−799.
(32) J. G. Deng, G. Su, P. Chen, Y. Du, Y. Gou and Y. Liu, *Inorg. Chim. Acta*, 2018, **471**, 194−202.
(33) M. Niu, H. Li, X. Li, J. Dou and S. Wang, *RSC Adv*., 2015, **5**, 37085−37095.
(34) J. Haribabu, K. Jeyalakshmi, Y. Arun, N. S. P. Bhuvanesh, P. T. Perumal and R. Karvembu, *RSC Adv*., 2015, **5**, 46031−46049.